Indian Journal of Chemical Technology
Vol. 29, November 2022, pp. 713-720
DOI: 10.56042/ijct.v29i6.67423

Synthesis and characterization of graphene nanosheets for electrochemical quantification of chlorpheniramine maleate drugs using a modified glassy carbon electrode

E Murugan*, A Poongan, M Kesava & A Vinitha

Department of Physical Chemistry, School of Chemical Sciences, University of Madras, Chennai 600 025, Tamil Nadu, India.
E-mail: dr.e.murugan@gmail.com

Received 19 August 2022; accepted 21 October 2022

The development of innovative sensors for the detection of analytes at extremely low concentrations with great sensitivity and selectivity has been a major focus of this study. The electrochemical activity of chlorpheniramine maleate (CPRM) in the presence of a graphene modified GCE has been investigated. Cyclic voltammograms (CV) have been obtained in the linear dynamic range 3.5- 156 µM while the optimum *p*H range and the maximum peak current (IPa) have been measured at *p*H 7.3. The process on the electrode's surface, diffusion regulated, heterogeneous rate constant, charge transfer coefficient, and the number of electrons transferred among the physicochemical properties have been obtained. Differential pulse voltammetry (DPV) of CPRM at the modified has electrode revealed a good linear calibration curve with a linear range of 10 to 60 µM and limit of detection of 0.062 µM. The suggested sensor has been fabricated and utilized to determine CPRM in medicines as well as serum samples.

Keywords: Chlorpheniramine maleate, Electrochemical sensor, Graphene@GCE, Ullman method

Chlorpheniramine maleate (CPM), also known as 3- (4- chloro, phenyl)-n, n- dimethyl- 3- pyridin-2-yl propan-1-amine (Structure 1), is a well-known antihistamine that is commonly used to treat common colds and allergy disorders, both alone and in conjunction with other drugs[1-3]. Common adverse effects include drowsiness, constipation, dizziness, blurred vision, hallucinations, anxiety, disorientation, nausea, dry mouth, restlessness, poor coordination, shallow breathing, irritability, tinnitus, memory or concentration disorders, and trouble urinating. As a result, multiple approaches for its detection in pharmaceutical dosage form and biological fluids have been developed, including spectrophotometry[4], chromatographic methods such as HPLC[5-9], LC-MS[10], RP-HPLC[11-13], and LC-MS-MS[14-16]. Other analytical methods, such aselectrophoresis[17,18], chemiluminescence[19,20], and capillary electrogenerated chemiluminescence[21,22], have been used to quantify CPRM in drug preparations. CPRM has also determined electrochemically using modified glassy carbon[23-25] and carbon paste electrodes[26-28].

Graphene nanosheets are a popular material for use as filler in electrochemical applications because of its exceptional qualities like as strong thermal and mechanical strength, huge surface area, and easy functionalization possibilities[28]. In this study, crucial and incredibly stable graphene nano sheet is employed for the first time to detect CPRM electrochemically. The analytes employed in this investigation have multiple functions. They have weakly and strongly interacting kinds with the electrode materials' surfaces. As a result, the needed surface must be highly heterogeneous in nature. Graphene, as everyone knows, is added to the matrix of electrode materials to improve electron capture and transport. Organics are not covalently bound to graphene in this case, but are simply distributed. Several researchers have performed a few types of electrochemical measurements using certain carbon materials. Some of them have performed caffeine sensor using graphene oxide[29-31], acetaminophen sensor using g-C_3N_4[32]and biosensor using MWCNT. But our innovative attempt is to measure electrochemical quantities with the help of CPRM with the electrode modified with only graphene produced by the Ullmann method at a scale that no researcher has ever thought of.

Experimental Section

Materials

Chlropharm, copper metal powder, HNO_3, chlorpheniramine maleate and NaH_2PO_4 and 0.1 M Na_2HPO_4 were received from SRL PVT Ltd.

Preparation of graphene nanosheets by a modified Ullmann method

Initially, 10 g of Cu powder and 25 mL of $CHCl_3$ were heated at 200°C for 10 h before being cooled to room temperature (RT) in a Teflon-lined autoclave (100 mL capacity). The obtained greenish black precipitates were treated with a 6 M HNO_3 solution at RT for 12 h and finally washed several times in DI water and filtered to eliminate water-soluble contaminants after drying in a vacuum at 100°C for 10 h, giving 0.9 g of pure Graphene nanosheet[33,34] (Scheme 1).

Fabrication of graphene modified GCE

Preceding the formation, GCE the surface was polished on a glass like surface and subsequently polished with fine grade alumina powders of 0.05-micron grain size. At that time, the electrode was washed with DI water and C_2H_5OH dried about at ambient temperature. At that time, 10 mg of graphene was scattered in 20 mL water. 5 µL of the suspension was taken from that stock solution, drop-casting onto the pre-treated GCE, and allowed to dry at ambient temperature to fabricated grapheme electrode; the control electrode was set up in a similar manner.

Pharmaceutical preparation procedures

Mortar was used to grind five pieces of CPRM tablets. In a 100 mL calibrated flask, a weight matching to the stock solution was taken and brought to volume with double deionized. After 10 min of sonication, the solution was diluted in buffer solution (*p*H = 7.3) to achieve the appropriate concentration. The solution was investigated using the usual addition approach. The recovery studies were carried out using the conventional addition approach. The drug content of the tablet was determined using the regression analysis or calibration graph.

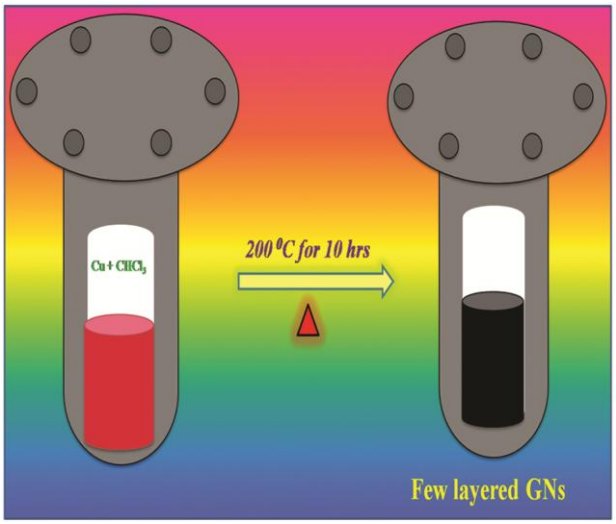

Scheme 1 — Synthesis of few layered graphene nanosheets using Ullmann method.

Human urine and serum analysis

The urine of four healthy participants of the same age group and gender was collected. Aliquots were centrifuged at RT (25 0.1 0104°C) for five minutes at 7000 rpm, and urine samples were either analyzed immediately or kept at a low temperature till analysis. Serum samples from healthy patients were refrigerated until the test, and an aliquot was fortified with CPM to generate a final concentration of 1.0 mM. The same serum sample was treated with 0.4 mL of acetonitrile and the volume was increased to 3.0 mL while the liquid was vortexed for one minute before centrifuging for ten minutes at 4000 rpm to remove the protein residues; finally, the *p*H=7.3 analysis and quantification were performed using the calibration plot method.

Instrumentation

The PXRD was taken using Cu K radiation (1.54), and the diffractometer X-ray tube current and voltage were adjusted to 30 mA and 40 kV, respectively. The morphology of graphene nanosheets was studied using the FEI-TECNAI T20 high resolution transmission electron microscopy (HR-TEM). The FT-Raman spectrum was captured with a Witec Confocal Raman apparatus and an Ar ion laser (514.5 nm) (CRM200). The HR-SEM was powered by a 200 keV with accelerating voltage and an energy dispersive X-ray analysis (EDX) system. At RT, FT-IR from 400 to 4000 cm^{-1} was collected using a Bruker spectrometer. A CHI 1130a electrochemical workstation (CH Instruments) was used for all electrochemical investigations.

Results and Discussion

High resolution scanning electron microscope (HR-SEM)

Figure 1 depicts the surface microstructure of graphene nanosheets. The SEM images clearly show that graphene nano sheets had a folded thin layer with some wrinkles. Furthermore, the chemical contents of produced graphene nanosheets were determined using an EDX spectrum, as shown in Fig. 1. The EDX studies revealed just carbon, oxygen, and chlorine (Cl), confirming the purity of the GNs while also revealing the chlorine, which is owing to the inadequate dechlorination process of GNs synthesis *via* the Ullmann reaction.

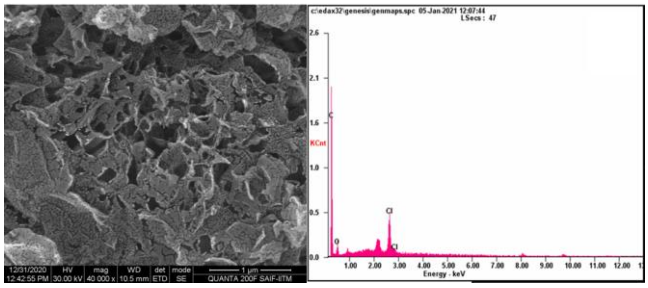

Fig. 1 — HR-SEM images of graphene nanosheets with EDAX spectrum.

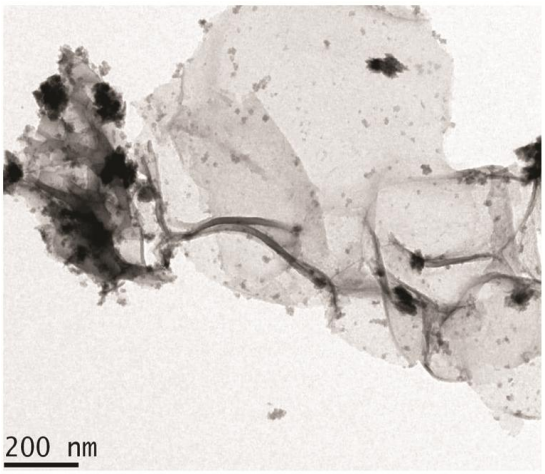

Fig. 2 — HR-TEM image of graphene nanosheet.

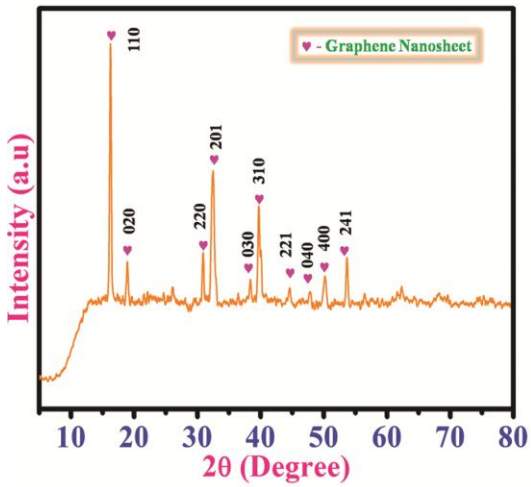

Fig. 3 — PXRD analysis of few layered graphene nanosheets.

High resolution transmission electron microscope (HR-TEM)

The graphene nanosheet were made using the hydrothermal technique and the Ullmann reaction; the precipitates were then treated with conc. HNO_3 to remove copper chloride (a by-product) and, lastly, to generate pure graphene nanosheet. HR-TEM images, as shown in Fig. 2, confirmed the morphology of the prepared graphene nanosheet. The prepared graphene nanosheet had a big, chaotic, sheet structure with wrinkles, indicating that the graphene nanosheet was successfully prepared, and the results were also consistent with HR-SEM pictures as seen in Fig 1.

PXRD, FT-IR and Raman analysis of graphene nanosheets

PXRD was used to investigate the crystallographic character of the graphene nanosheet, and the observed patterns are displayed in Fig. 3. The graphene nanosheets diffraction peaks at 2θ = 17.16° (110), 19.13° (020), 31.25° (220), 32.98° (201), 37.95° (310), 40.25° (221), 45.52° (040), 49.3° (400), 53.62° (241), shown in Fig. 3. Some of the most notable are very sharp peak locations such as 2 = 17.16° (110) and 32.98° (201)[30], indicating that the graphene nanosheet have a structure that is between semi-

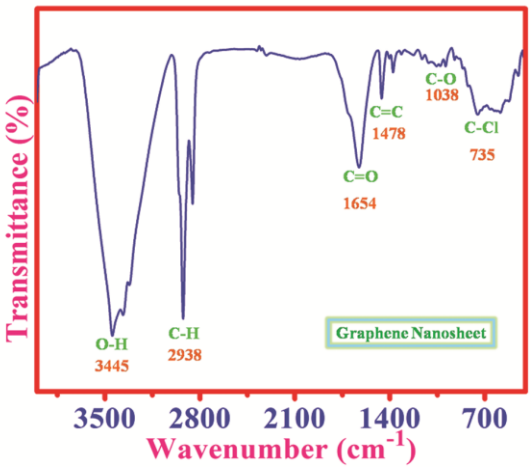

Fig. 4 — FT-IR analysis of few layered graphene nanosheets.

crystalline and amorphous. Furthermore, the very weak peak identified at 45.52° (040), indicating that Cu was unable to generate single-layered graphene nanosheet; they were composed of several layers.

Peaks at 2938 and 3445 cm^{-1} in Fig. 4 were caused by C-H and O-H stretching, respectively. The C=O and C=C stretching's occurred at 1654 and 1478 cm^{-1}.

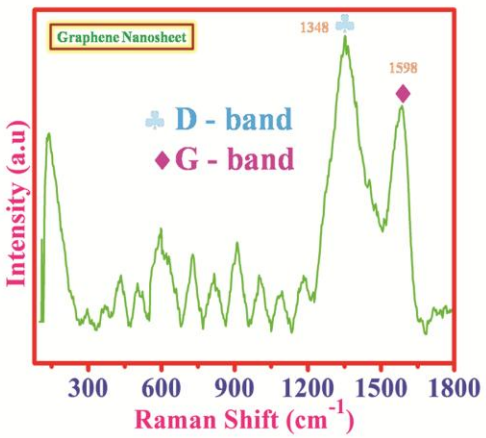

Fig. 5 — Raman analysis of few layered graphene nanosheets.

The C-O stretching mode was related to the band within this 1038 cm^{-1} range, and surface functionalization with -COOH, -OH, -COOC-, and -C-O-C- happened even during the post-synthesis chemical process. Another well-known method for producing surface oxygen functionality is nitric acid treatment, with poor adsorption at 735 cm^{-1} indicating the existence of covalently attached chlorine groups[31]. Raman spectral analysis (Fig. 5) depicts four typical peaks in the 1200-1700 cm^{-1} range. Because of the inclusion of the sp^3 character, the topological faults or disorder of the generated s were attributed to the peak of about 1348 cm^{-1}, D-band. The peak at 1598 cm^{-1} was noticed as a result of the increased sheet thickness, and it is known as the G-band[32].

Electrochemical behaviour of bare and graphene modified electrodes for detection of CPRM

Cyclic voltammetry using 0.1 M phosphate buffer solution (*p*H 7.3) at a 50 mV s^{-1} scan rate in the presence of CPRM was used to investigate the electrochemical behaviour of several electrodes, including bare GCE and GCE@graphene (Fig. 6). The CPRM concentration was 20 µM, and the peak current and peak potential were both high for the modified GCE@graphene compared to the naked electrode. It was discovered that the CPRM oxidation peak utilizing GCE@graphene occurred at 7.4 V, which is lower than the bare GCE (3.8 V). At the same time, CV was used to investigate the electrocatalytic activity of GCE@graphene at varied CPRM concentrations ranging from 0.10 to 60.6 M (Fig. 7).

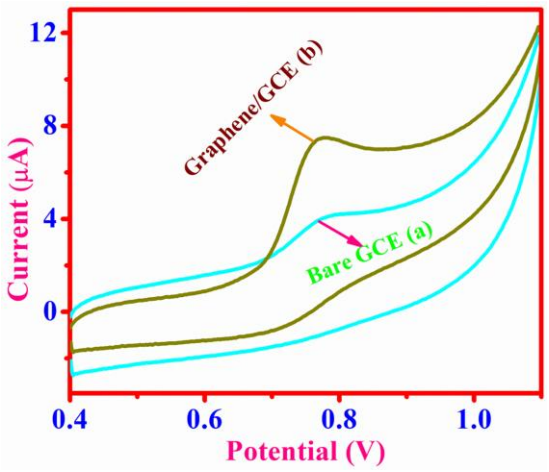

Fig. 6 — Cyclic voltammogram in the presence of 0.1 mM of 10 µM CPRM (a) bare GCE and (b) graphene@GCE in phosphate buffer solution *p*H 7.3 at a scan rate of 50mVs^{-1}.

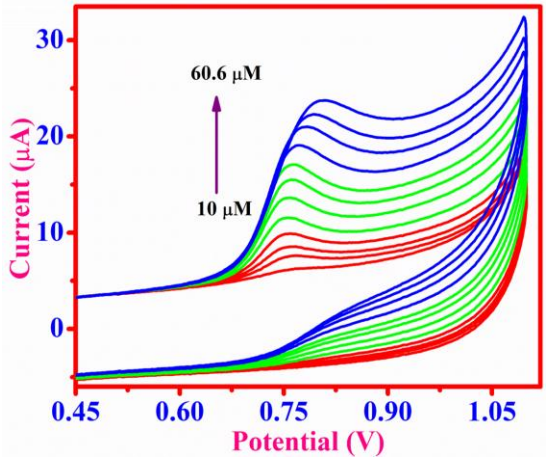

Fig. 7 — Cyclic voltammogram in the presence of 0.1 mM CPRM, at the Graphene@GCE in phosphate buffer solution *p*H 7.3 at a scan rate of 50mVs^{-1} and the linear range 10 to 60.6 µM.

Influence of scan rate on Graphene@GCE modified electrode

The influence of scan rate on peak current was investigated using 0.1 M PBS with a *p*H of 7.4, 0.1 mM, and 20 µM CPRM at different scan rates 10, 20, 30, 40, 50, 60, 70, 80, 90, and 100 mV s^{-1}. Examining the scan rate impact is crucial in the analysis of many physicochemical characteristics, and the peak current equals the voltammetric scan rate used. The slope of log IP as a function of the log was 0.613, very near to the expected value of 0.5 for diffusion-controlled systems,[33,35] [Fig. 8(b)] according to the equation;

$$\log Ip = 0.6313 \log \upsilon + 1.049 \quad \ldots(1)$$

$$R^2 = 0.9987 \quad \ldots(2)$$

Meanwhile, when the scan rate rose, the oxidation peak (Epa) became positive. The movement of two electrons and protons occurred during the oxidation of CPRM. The proposed electrochemical oxidation mechanism of CPRM is illustrated Scheme 2.

Influence of *p*H on GCE@graphene modified electrode

Proton is always present in organic compounds electrochemical reaction and had a substantial impact on the reaction speed. As a result, the effects of solution *p*H on the CPRM electrode reactivity were measured in the *p*H range 3.0 - 11.0 at a chosen scan rate of 0.05 Vs^{-1} [Fig. 9(a)]. A minor peak was found in the *p*H range 3.0 to 5.0 as the solution *p*H increased. From *p*H 6.0 to 11.0, the potentials of the peaks were moved to fewer positive values. The slope of 62 mV/*p*H for an equal number of electrons and proton transfer [Fig. 9(b)] agrees well with the Nernstian value of 59.0 mV/*p*H for the same amount of electrons and proton transfer (Fig. 9a)[36] with linear equation:

$$Ep = 0.048\ pH + 1.09 \quad \ldots(3)$$

$$R^2 = 0.9976 \quad \ldots(4)$$

According to the plot of peak current as a function of *p*H, the maximum peak current was attained at *p*H 7.3.

Oxidation mechanism

The anodic peak on a forward scan suggested CPRM oxidation, but no any peak was identified on a reverse scan; hence, the results in this irreversible system imply two-electron transfer mechanisms involved in CPRM oxidation, as depicted in Scheme 2.

Determination of the magnitude of CPRM based on the differential pulse voltammetry

The differential pulse voltammetry (DPV) approach is typically more sensitive to CV. As a result, this method might be utilized to detect CPRM quantitatively at graphene-modified GCE under ideal

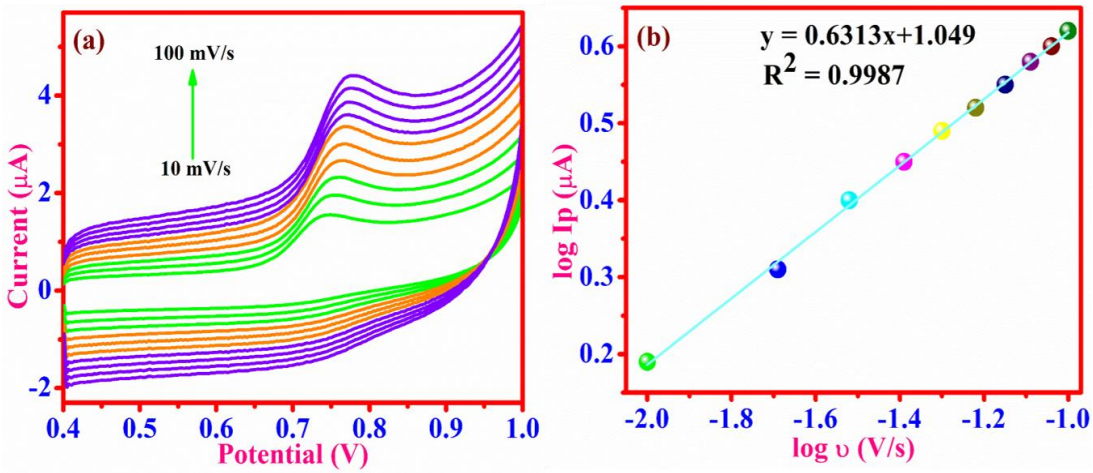

Fig. 8 — (a) Effect of the scan rates on the cyclic voltammetric responses in buffer solution of *p*H 7.3 at the graphene@GCE for 0.1 mM CPRM at various scan rates (from 10 to 100): 10, 20, 30, 40, 50, 60, 70, 80, 90 & 100 mV s^{-1} and (b) The relationship of anodic peak currents and the scan rate for CPRM (0.1 mM).

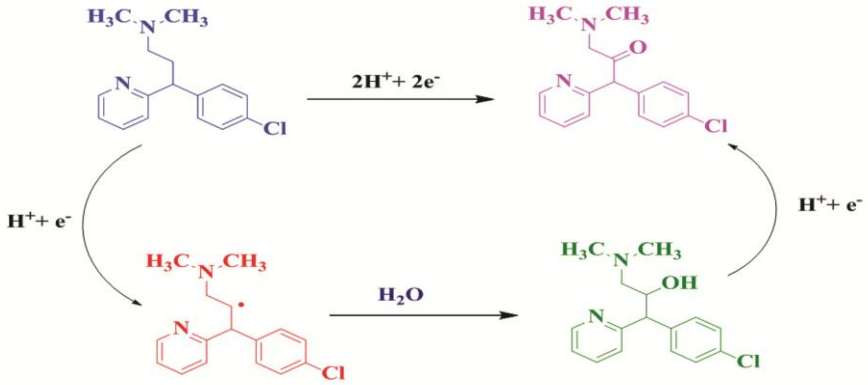

Scheme 2 — Possible electrode oxidation reaction mechanism of CPRM.

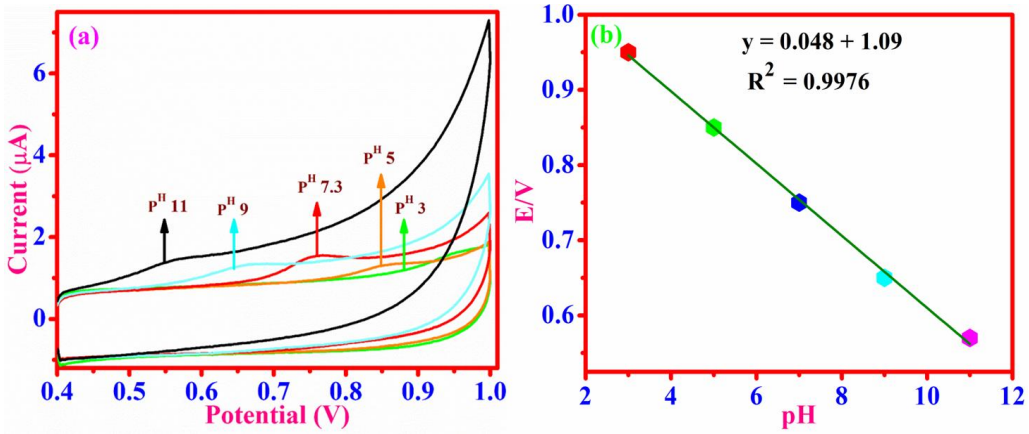

Fig.9 (a) — Cyclic voltammograms of 0.1mM CPRM at the surface of the graphene@GCE immersed in in phosphate buffer solution *P*H 3-11, scan rate 50 mV/s and (b) variation of anodic peak potential verses. various *p*H values in 0.1 mM CPRM.

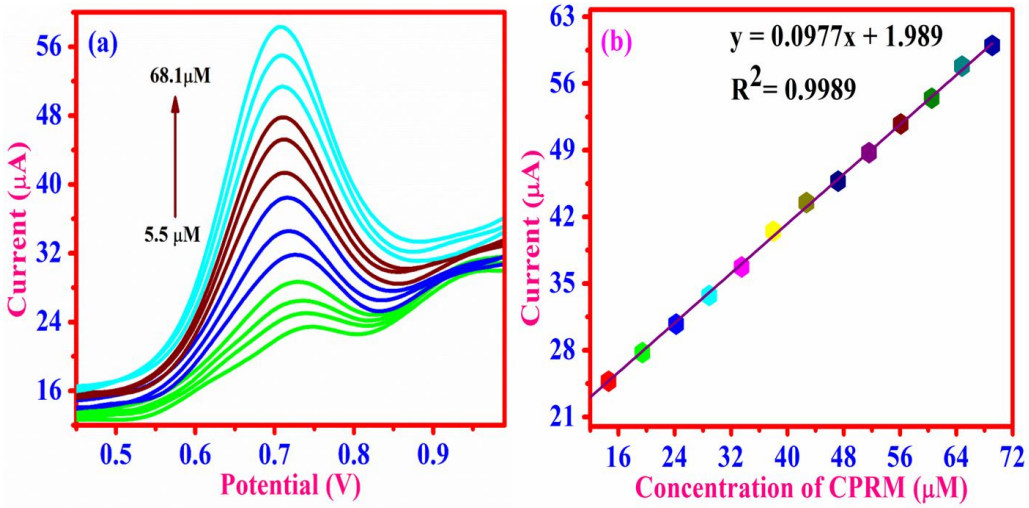

Fig. 10 — (a)DPVs of 5.5to 68.1μM CPRM on the graphene@GCE under the optimum conditions and a scan rate of 50mVs^{-1} and (b) Plot of the peak current in differential pulse voltammetry versus the concentration of CPRM.

circumstances with a scan rate of 50 mVs^{-1}. Figure 10(a) depicts a DPV reaction to the addition of CPRM. According to the findings, a well-defined reaction was found with the sequential addition of CPRM. The response current, as observed, is linear in the CPRM concentration range of 5.5 to 68.1 μM, with the linear equation

Ipa/A = 0.0977 [CPRM]/μM + 1.989 …(5)

R2 = 0.9989 …(6)

A correlation coefficient of 0.9989 was obtained [Fig. 10(b)], indicating that the regression line extremely well fits the experimental data and that the regression equation may be utilized to predict the unknown sample.

Interference study

The current study looked at how different substances affected the measurement of 50 μM CPRM under ideal conditions. The tolerance limit was established as the greatest concentration of the interfering material that caused a less than 5% error in CPRM determination, and the results demonstrated that the presence of these coexisting species had no influence on the current response of 100 M CPRM.

Modified electrodes of reproducibility and stability

The reproducibility of 5 replicate assessments of 20 μM CPRM was studied, yielding a relative standard deviation (R.S.D.) of 1.96%. Table 1 compares the findings of this study to previously published voltammetric techniques for evaluating CPRM, and the analytical features are equivalent or superior to those reported for CPRM measurement at the surface of other modified electrodes, as seen.

The graphene-modified GCE was stable in 0.1 M buffer solution at 4°C for two weeks, with no obvious changes in the present response when using the same

Table 1 — Comparison of limit of detection and linear range of CPRM by electroanalytical methods.

Various electrodes	Drugs	Technique	Limit of Detection (μM)	Linear range (μM)	Ref.
Ru/Pty/GCE	CPRM	CV	0.338	2.0-45	[37]
CPE/SDS	CPRM	DPV	1.7	1.0-800	[38]
MWCNT-modified GCE	CPRM	DPV	1.63	5.0-500	[39]
CPE-Co nanostructure	CPRM	DPV	0.08	0.1-10	[40]
SDS/GCE	CPRM	SWV	0.028	0.1-100	[41]
HMDE	CPRM	SWV	0.984	0.98-9.75	[42]
Graphene Nanostructure/GCE	CPRM	DPV	0.062	5.5-68.1	This work

Table 2 — Application of DPV for the determination of CPRM in spiked blood andhuman urine.

S. No	Samples	Added (μM)	Found[a] (μM)	Recovery (%)	RSD %
1	Blood	5	4.99	99.5	2.25
2	Urine	10	9.85	98.1	2.35
3	Urine	20	19.95	99.0	2.28

[a]Mean value n = 3

sample concentration. After three weeks, the current responses for detecting 20 M of CPRM decreased by less than 5% of the original response, indicating that the suggested electrode's durability was adequate for electrochemical applications.

Analysis of CPRM in serum, drug samples

The calibration plot was used to assess the unknowns after drug-free urine samples were spiked with a known dosage of the drug. The ease of assessing CPRM was only achievable due to the method's simplicity and the absence of a pre-extraction process for urine samples. Subsequently, the results of recovery investigations revealed that amazing recoveries ranged from 99.0% to 99.5%, with a percentage of RSD of 2.25%. (Table 2). Furthermore, the acquired results provided a clear indication of the method's suitability for determining CPRM from genuine biological matrices. The process for spiked human serum samples with the analyte has been previously discussed in pharmaceutical preparation procedures. The recoveries in various samples were found to be between 98.0% and RSD is found to be 2.35%.

Conclusion

In conclusion, it has been demonstrated that the oxidation behaviour of CPRM on graphene-modified GCE, significantly improved the electrochemical performance of CPRM and clearly demonstrates the graphene@GCE's better electrocatalytic activity toward CPRM oxidation. Under ideal circumstances, the oxidation peak current is proportional to CPRM concentration in the range of 5.5-68.1 μM, with a detection limit of 0.062 μM, indicating that the modified electrode is successful in detecting CPRM in actual samples with high sensitivity. The study findings allow us to conclude that DPV may be used to quantitatively identify these drugs alone or in combination, as is commonly done in pharmaceutical formulations, with various advantages. The graphene @GCE's high sensitivity can be due to its enormous surface area. It has great stability, a lower detection limit, a wide linear dynamic range, excellent catalytic activity, and repeatability. Graphene@GCE has provided considerable benefits by combining exceptional conductivity and unique properties.

Acknowledgement

RUSA-2.0/RI&QI-Govt. of India/TN Govt., University of Madras, and Chennai provided financial support to the authors.

References

1 El-Maali A N, *Bioelectrochem*, 64 (2004) 99.
2 A l Lawati H, Suliman F, A l Kindy S, Al-Lawati A, Varma G & Nour I, *Talanta*, 82 (2010) 1999.
3 Murugan E & Pakrudeen I, *Sci Adv Mater*, 7 (2015) 891.
4 Erk N, *J Pharmaceut Biomed Anal*, 23 (2000) 1023.
5 Heydari R, *Anal Lett*, 41 (2008) 965.
6 Amer S M, Abbas S S, Shehata M A & Ali N M, *J AOCA Int*, 91 (2008) 276.
7 Palabiyik M & Onur F, *Chromatographia*, 66 (2007) 93.
8 Marin A & Barbas C, *J Pharm Biomed Anal*, 35 (2004) 769.
9 Moyano M A, Rosasco M A, Pizzorno M T & Segall A I, *J AOCA Int*, 88 (2005) 1677.
10 Hao L, Chao Z, Jiang W, Yao J, Paul F & Jingkai G, *J Pharm Biomed Anal*, 51 (2010) 716.
11 Martinez-Algaba C, Bermudez-Saldana J M, Villanueva-Camanas R M, Sagrado S & Medina-Hernandez M J, *J Pharm Biomed Anal*, 40 (2006) 312.
12 Murugan E, Priya A R J, Janakiraman J & Kalpana K, *J Nanosci Nanotechnol*, 19 (2019) 7596.

13 Erdal D, Abdil O, Halil A, Ozgur U & Dumitru B, *Chem Pharm Bull*, 54 (2006) 415.
14 Liao Q, Xie Z, Pan B, Zhu C, Yao M, Xu X & Wan J, *Chromatographia*, 67 (2008) 687.
15 Murugan E, Yogaraj V, Rani D P G & Sinha A K, *RSC Adv*, 5 (2015) 106461.
16 Celma C, AllueJA, Pruonosa J, Peraire C & Obach R, *J Chromatography*, 870 (2000) 77.
17 Dong Y, Chen X, Chen Y, Chen X & Hu Z, *J Pharmaceut Biomed Anal*, 39 (2005) 285.
18 Suliman F E, Al-Hinai M M, Al-Kindy S M & Salama S B, *Luminescence*, 24 (2009) 2.
19 Yogaraj V, Gautham G, Akshada C, Manikandan R & Murugan E, *J Drug Deliv Sci Technol*, 58 (2020) 101785.
20 Murugan E & Akshata C R, *Adv Mater Proc*, 2 (2017) 176.
21 Song H, Zhang Z &Wang F, *Electroanalysis*, 18 (2006) 1838.
22 Murugan E & Kalpana K, *Adv Mater Proc*, 3 (2018) 75.
23 Muralidharan B, Gopu G, Laya S, Vedhi C & Manisankar P, *Mat Sci Appl*, 2 (2011) 957.
24 Murugan E, Rani D P G & Yogaraj V, *Colloids Surf B: Biointerfaces*, 114 (2014) 121.
25 Lamani S D, Hegde R N, Savanur A P & Nandibewoor S T, *Electroanalysis*, 23 (2011) 347.
26 Murugan E, Rani D P G, Srinivasan K & Muthumary J, *Expert Opin Drug Deliv*, 10 (2013) 1319.
27 Abu-Shawish H M, *Electroanalysis*, 20 (2008) 491.
28 Murugan E & Kumar K, *Anal Chem*, 91 (2019) 5667.
29 Murugan E & Poongan A, *Indian J Chem Tech*, 28 (2021) 528.
30 Murugan E, Dhamodharan A, Poongan A & Kalpana K, *Indian J Chem Section A*, 59 (2020) 1313.
31 Murugan E & Poongan A, *Diam Relat Mater*, 126 (2022) 109117.
32 Murugan E, Poongan A & Dhamodharan A, *J Mol Liq*, 348 (2022) 118447.
33 Sawant S Y, Somani R S, Cho M H & Bajaj H C, *RSC Adv*, 5 (2015) 46589.
34 Kesava M, Saravanan V, Srinivasan K & Dinakaran K, *Int J Energy Res*, (2022) 1-17.
35 Sawant S Y, Somani R S, Sharma S S & Bajaj H C, *Carbon*, 68 (2014) 210.
36 Srinivas G, Zhu Y, Piner R, Skipper N, Ellerby M & Ruoff R, *Carbon*, 48 (2010) 630.
37 Gosser D, "Cyclic Voltammetry: simulation and analysis of reaction mechanisms," Vancouver Coastal Health, New York. (1993).
38 Bukkitgar S D, Shetti N P, Kulkarni R M, Halbhavi S B, Wasim M, Mylar M, Durgi P S & Chirmure S S, *J Electroanal Chem*, 778 (2016) 103.
39 Nayak D S & Shetti N P, *J Anal Sci Technol*, 7 (2016) 1.
40 Khudaish E, Al-Hinaai M, Al-Harthy S & Laxman K, *Electrochim Acta*, 135 (2014) 319.
41 Lamani S, Hegde R, Savanur A & Nandibewoor S, *Electroanalysis*, 23 (2011) 347.
42 Pourghobadi Z & Pourghobadi R, *Int J Electrochem Sci*, 10 (2015) 7241.